A Three-Dimensional Model of Lake Ontario's Summer Circulation. II. A Diagnostic Study[1]

JOHN R. BENNETT

Environmental Research Laboratories, NOAA, Great Lakes Environmental Research Laboratory, Ann Arbor, MI 48104

(Manuscript received 6 February 1978, in final form 9 June 1978)

ABSTRACT

A two-layer circular lake model is used to study the mean flow of Lake Ontario during midsummer. By computing the model only to the second order of amplitude, it is shown that the observed cyclonic circulation of Lake Ontario during summer is due to the rectified effects of the large, transient, wind-driven currents. This effect is strongly influenced by model grid resolution and friction.

1. Introduction

Part I of this study (Bennett, 1977) presented a numerical model which improves the simulation of Lake Ontario currents. My purposes here are to analyze the reasons for the improvement and, by doing so, to determine whether they are unique to Lake Ontario or not. I will do this by studying a circular two-layer model that includes the most essential features of the numerical model but that is easier to understand. I will only discuss the time-averaged flow, but I will not assume the flow is steady. For the two-layer model, the response to a steady uniform wind is the "static" solution of thermocline setup. Since this solution only occurs after many months of steady winds and does not look like either the observed or the numerical model's time-averaged flow, the analysis must be transient.

To summarize the observed flow, Fig. 1 gives the thermocline depth and longshore volume transport estimated from Csanady and Scott's (1974) daily synoptic surveys for 15 July–15 August 1972. Except for an upwelling region near the northwest shore, the thermocline is deeper at the shore than in mid-lake and there is a cyclonic circulation. During this period the average wind stress is toward the east at about 0.15 dyn cm^{-2} and is relatively uniform over the lake. There are periods of a few days when the stress is as high as 1 dyn cm^{-2}.

The numerical model reproduces the observed thermocline shape and currents relatively well if the shore zones are adequately resolved and friction is small. However, the simulations were begun with the shore water warmer than the deep water, a pattern that causes a cyclonic circulation. Thus, the simulation with lower friction may be better partly because the thermal circulation decays slower.

The rectified effect of the large wind-driven upwellings and downwellings of the thermocline is important in causing the cyclonic flow. This is the most important nonlinearity in the model since momentum advection is neglected. Cross-sectional models (Bennett, 1975a,b) have shown that it is the right sign and magnitude for Lake Ontario. Moreover, Simons (1975) showed that the same is true for a three-dimensional model. Thus, the questions to be answered here pertain not to whether or not the effect occurs but to how it depends on the coefficients of friction, on the model resolution and on bottom topography. I want to determine under what conditions the effect can be increased and whether it can be explained in simpler terms than before.

I will first examine a very simple model in Section 2. Then, in Sections 3 and 4 I will analyze the circular model in detail. Finally, in Section 5 I will summarize both parts of this paper as well as the Bennett and Lindstrom (1977) paper.

2. A very simple model

To illustrate the mechanism, we suppose 1) friction is negligible; 2) the lower layer is infinitely deep; 3) all longshore variations are neglected and the coast is straight; 4) the wind stress is uniform, parallel to shore and constant in time; and 5) the longshore component v of the current is geostrophic.

The equations are

$$-fv + g' \frac{\partial h}{\partial x} = 0, \tag{2.1}$$

$$\frac{\partial v}{\partial t} + u \frac{\partial v}{\partial x} + fu = \frac{\tau_y}{\rho_0 h}, \tag{2.2}$$

[1] Great Lakes Environmental Research Laboratory Contribution No. 124.

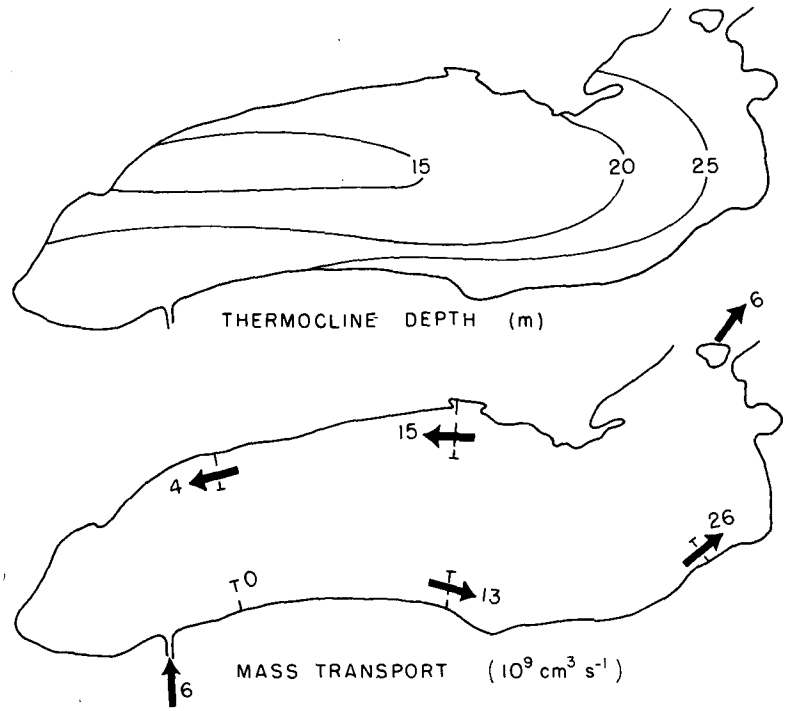

FIG. 1. Lake Ontario thermocline depth and mass transport (15 July–15 August 1972) estimated from daily synoptic surveys at five transects.

$$\frac{\partial h}{\partial t} + \frac{\partial}{\partial x}(uh) = 0. \tag{2.3}$$

If at $t = 0$ the longshore current is zero, the thermocline is level at a depth H and there is a wall at $x = 0$, the initial and boundary conditions are

$$\left.\begin{aligned} &t = 0, && v = 0, \quad h = H \\ &x = 0, && u = 0 \\ &x \to -\infty, && h \to H \end{aligned}\right\}.$$

If the right-hand side of (2.2) were constant the thermocline depth would be

$$h = H + [\tau_y t/\rho_0(g'H)^{1/2}] \exp[xf(g'h)^{-1/2}]. \tag{2.4}$$

This is the familiar coastal jet solution for which the potential vorticity is uniform (Charney, 1955). It is possible to solve this problem even with the longshore derivative terms in (2.2) and (2.3) (Bennett, 1973). However, the effective acceleration $\tau_y/\rho_0 h$ is not a constant; its variation is as important as that of the other nonlinear terms.

To analyze this effect, we assume the solution can be written as a power series in t, i.e.,

$$\left.\begin{aligned} u &= u_1 + u_2 t + \ldots \\ v &= v_1 t + v_2 t^2 + \ldots \\ h &= H + h_1 t + h_2 t^2 + \ldots \end{aligned}\right\}.$$

These forms satisfy the initial conditions. If they are inserted in Eqs. (2.1)–(2.3) and like powers of t are equated, the resulting thermocline displacement is

$$h = H + [\tau_y t/\rho_0(g'H)^{1/2}] \exp[xf(g'h)^{-1/2}] - \tfrac{1}{4}(\tau_y^2 t^2/\rho_0^2 g' H^2)\{[xf/(g'h)^{1/2}] + 1\} \times \exp[xf(g'h)^{-1/2}]. \tag{2.5}$$

The difference between this and (2.4) is negative closer to shore than the radius of deformation and positive further from shore. At the shore it increases upwellings and decreases downwellings. The thermocline shapes predicted by the constant potential vorticity theory (2.4) and the complete second-order theory (2.5) are given in Fig. 2 for a wind impulse that, according to linear theory, should cause a maximum vertical displacement of three-fourths the original thermocline depth.

If this same problem is done without the inertial acceleration term $u\partial v/\partial x$, or for a finite lower layer depth, the result is not qualitatively different—the upwelling is larger than the downwelling. We can use this simple fact to understand the following more realistic model.

Imagine a perfectly circular body of water bounded by a rigid surface and a bottom for which the depth is only a function of radius. If there is no bottom stress and no wind stress curl, the angular momentum of the whole lake cannot change with time. In addition, without inertial accelerations the angular momentum contained between any two radii is also constant. If such a lake is initially at rest, no matter what the internal density distribution is or how the wind changes with time, the average of the

mass transport streamfunction around any radius is always zero.

Now suppose the lake has a shallow thermocline and is subject to wind impulses from random directions. Because the upwellings of the thermocline would be larger than the downwellings, the net effect of many impulses would be to cause a mean upwelling near the shore and a compensating depression in the center. Thus, the lower layer must move outward, and if there is no stress across the thermocline, it must spin anticyclonically to conserve its angular momentum. Bottom friction acting on this current will cause a net gain of cyclonic angular momentum.

3. Description of the circular lake model

Since the purposes of these calculations are to isolate this effect, and also to evaluate the numerical method of Part I, they are designed so that:

1) Only *forced* waves can generate a circulation with radial symmetry; instabilities of the symmetric flow are not allowed.

2) It uses the most important features of the numerical method—increased coastal resolution and smoothing of the horizontal divergence field.

Fig. 3 defines the variables of the model. As in the numerical model of Part I, the hydrostatic, Boussinesq and rigid-lid approximations are used. The interface and bottom stresses are linearly proportional to the shear and the bottom current:

$$\tau_i = \rho_0 c(\mathbf{V}_1 - \mathbf{V}_2), \tag{3.1}$$

$$\tau_b = \rho_0 d\mathbf{V}_2. \tag{3.2}$$

It is convenient to write the equations in terms of the current shear across the thermocline and the streamfunction Ψ. Using the definitions

$$u = u_1 - u_2, \quad [u_1 h + u_2(D-h)]/D = -\frac{1}{rD}\frac{\partial \Psi}{\partial \theta},$$

$$v = v_1 - v_2, \quad [v_1 h + v_2(D-h)]/D = \frac{1}{D}\frac{\partial \Psi}{\partial r},$$

$$Z = \frac{\partial}{\partial r}\frac{r}{D}\frac{\partial \Psi}{\partial r} + \frac{1}{rD}\frac{\partial^2 \Psi}{\partial \theta^2},$$

$$g' = g\frac{\Delta \rho}{\rho_0},$$

$$AU_i = u_i\frac{\partial u_i}{\partial r} + \frac{v_i}{r}\frac{\partial u_i}{\partial \theta} - \frac{v_i^2}{r},$$

$$AV_i = u_i\frac{\partial v_i}{\partial r} + \frac{v_i}{r}\frac{\partial v_i}{\partial \theta} + \frac{u_i v_i}{r},$$

$$N_u = -(h/D)AU_1 - [(D-h)/D]AU_2,$$

$$N_v = -(h/D)AV_1 - [(D-h)/D]AV_2,$$

$$a = \frac{cD + dD^{-1}h^2}{hD - h^2},$$

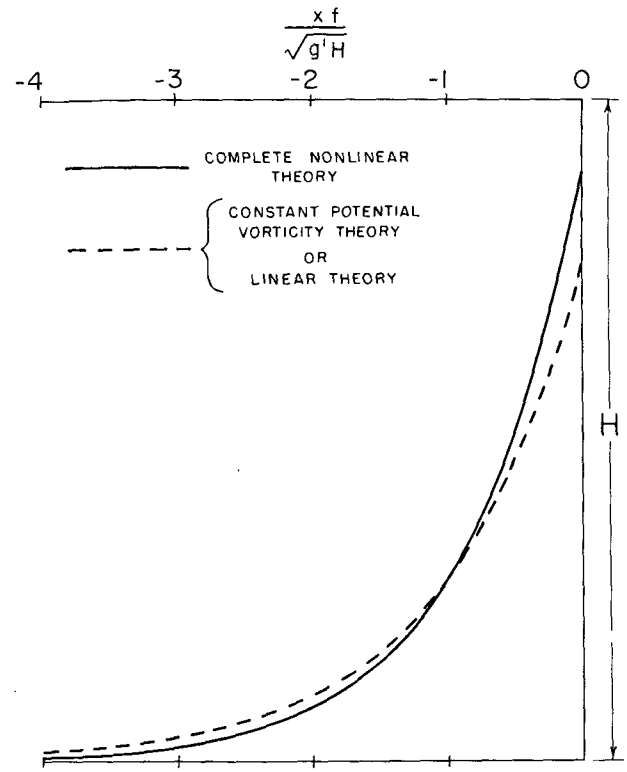

FIG. 2. Thermocline displacement in an upwelling zone for two inviscid theories.

the equations of the model are as follows:

$$\frac{\partial u}{\partial t} - fv + g'\frac{\partial h}{\partial r} = \frac{\tau_r}{\rho_0 h} - au - \frac{d}{rD(D-h)}\frac{\partial \Psi}{\partial \theta} - AU_1 + AU_2 \tag{3.3}$$

$$\frac{\partial v}{\partial t} - fu + \frac{g'}{r}\frac{\partial h}{\partial \theta} = \frac{\tau_\theta}{\rho_0 h} - av + \frac{d}{D(D-h)}\frac{\partial \Psi}{\partial r} - AV_1 + AV_2 \tag{3.4}$$

$$\frac{\partial h}{\partial t} + \frac{1}{r}\frac{\partial}{\partial r}(u_1 rh) + \frac{1}{r}\frac{\partial}{\partial \theta}(v_1 h) = 0 \tag{3.5}$$

$$\frac{\partial Z}{\partial t} + \frac{1}{D^2}\frac{\partial D}{\partial r}\frac{\partial}{\partial \theta}\left(f\Psi - g'\frac{h^2}{2}\right) = \frac{\partial}{\partial r}\left(\frac{\tau_{\theta r}}{D}\right) - \frac{1}{D}\frac{\partial \tau_r}{\partial \theta} - d\left[\frac{\partial}{\partial r}\left(\frac{rv_2}{D}\right) - \frac{\partial u_2}{\partial \theta}\right] + \frac{\partial}{\partial r}(rN_v) - \frac{\partial}{\partial \theta}N_u. \tag{3.6}$$

These equations were solved in two stages. First the solution of the linearized problem, which is separable in θ, is solved; this solution is then used to compute the second-order corrections. This

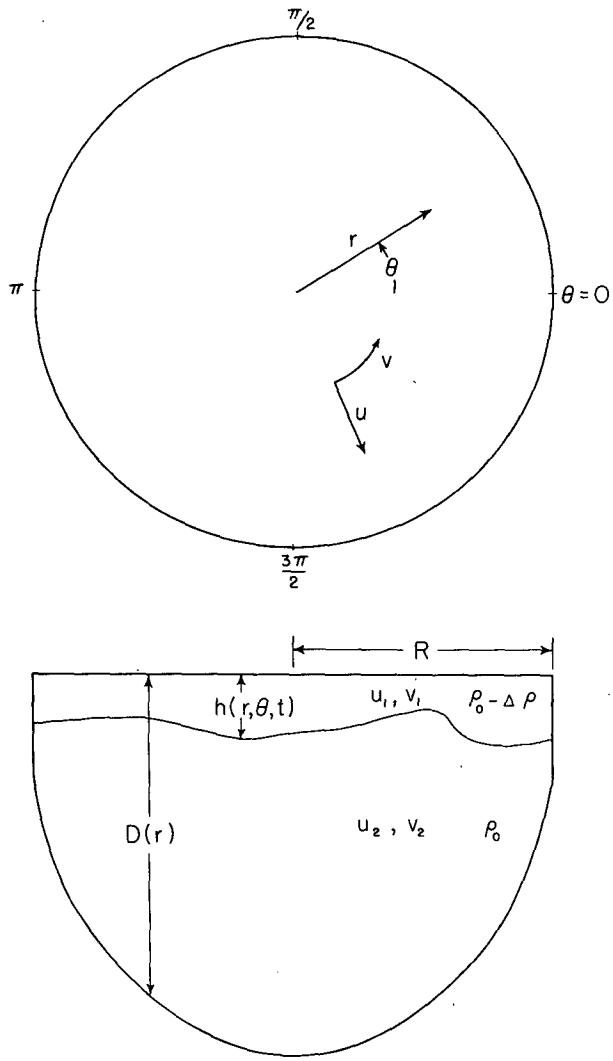

FIG. 3. Definition of terms for a circular lake model.

is equivalent to a low-order spectral model since in the computer program the solutions are calculated simultaneously. For a spatially uniform wind stress, the linear solution for any variable can be expressed in the form

$$h_{\text{lin}} = h_2(r,t)\sin\theta + h_3(r,t)\cos\theta. \quad (3.7)$$

The second-order solution is

$$h = h_1(r,t) + h_4(r,t)\sin 2\theta + h_5(r,t)\cos 2\theta. \quad (3.8)$$

The radius of the circular model is 75 km and the bottom is parabolic, rising from 141 m deep in the center to 32 m at the shore. The equilibrium depth H of the thermocline is 16 m and g' is 1.0 cm s^{-2}. As in Part I, the model was started from rest and driven by 46 days of wind stress estimated from Lake Ontario observations of 1 July to 15 August 1972. The thermocline displacement and streamfunction were then averaged over 15 July to 15 August. As a first choice the friction coefficients are

$$c = 0.001 \text{ cm s}^{-1}, \quad d = 0.02 \text{ cm s}^{-1}, \quad (3.9)$$

values suggested by the decay times of Bennett and Lindstrom's (1977) empirical model.

In addition, smoothing is incorporated into the numerical method. As in the numerical model of Part I, this smoothing applies only to the baroclinic mode and is equivalent to adding a term proportional to the horizontal divergence to the pressure. For this model, the baroclinic pressure gradient terms in (3.3) and (3.4) are evaluated with

$$h_{\text{smoothed}} = h - \frac{0.25f\Delta r^2}{gH}\frac{D}{D-H}\frac{\partial h}{\partial t}. \quad (3.10)$$

This smoothing term is proportional to f and Δr^2 so that it is formally the same order of error as the truncation error due to spatial averaging of the Coriolis term. There are 18 grid points spaced from 1.5 km apart nearshore to 9 km in the center, roughly the same resolution as in Part I. The numerical method is similar to the one used in the fully three-dimensional model, with a few modifications due to the polar coordinates. For these modifications I used Williams' (1969) technique. The computer program was tested by checking to see that it reproduced the cases of pure Kelvin wave and topographic wave propagation, and that it approached the steady-setup solution for a steady uniform wind. This last test is the most useful because for this solution the currents are zero and many programming errors or numerical instabilities cause the program to fail.

4. Solutions of the circular lake model

The solutions will be presented in three figures, each of which has three cases. Fig. 4 has cases with the same grid resolution and friction but with different degrees of nonlinearity. Fig. 5 compares cases with different values of bottom and interface friction. Fig. 6 compares cases of different grid resolution and smoothing. All cases are attempts at simulating the flow of Fig. 1, Lake Ontario's circulation averaged over 32 days, 15 July to 15 August 1972. In these figures, thermocline displacement in meters is on the left; to compare it with Fig. 1, one should add 16 m to the model solution. Streamfunction in units of 10^9 cm^3 s^{-1} is on the right hand side of Figs. 4–6. Except for the Niagara and St. Lawrence River flows, these numbers can be directly compared to the coastal transports of Fig. 1. All of these cases are simple variations of the one at the bottom of Fig. 4.

At the top of Fig. 4 is the solution to the completely linear problem. There is perfect radial symmetry; the thermocline is depressed downwind and

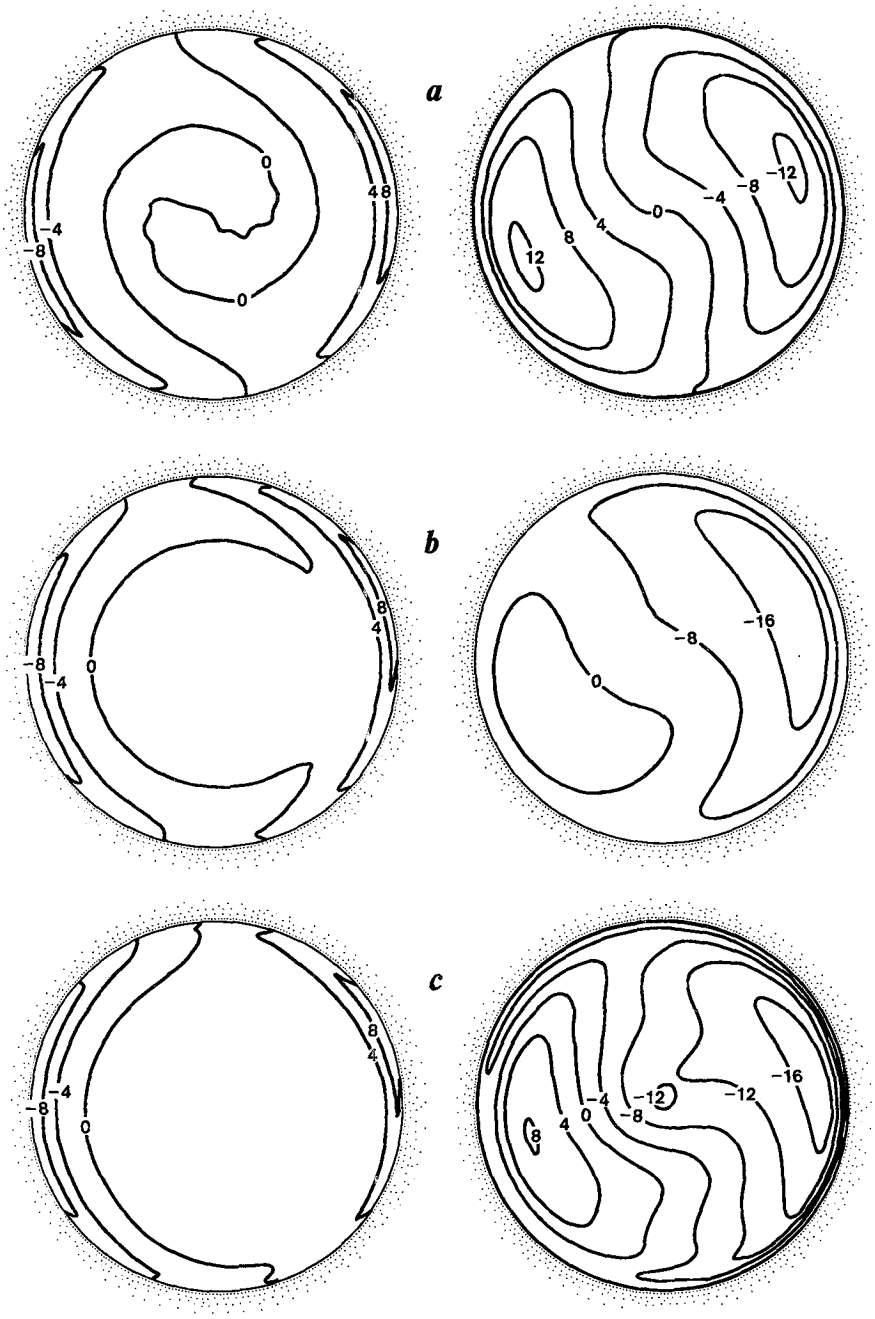

FIG. 4. Thermocline displacement (m) and streamfunction (10^9 cm^3 s^{-1}), 15 July to 15 August 1972, computed with interface friction of 0.001 cm s^{-1} and bottom friction of 0.02 cm s^{-1}: (a) linear theory, (b) second-order thermocline displacements and (c) second-order thermocline displacements plus the inertial acceleration terms.

has an equal upwelling at the western shore. The streamfunction field consists of equal cyclonic and anticyclonic gyres. In the central region the flow is to the right of the wind; and the return flow, to the left of the wind, occurs in narrow boundary currents. This pattern is similar to that predicted by Birchfield's (1972) theory for a homogeneous lake. However, due to stratification, the flow to the right of the wind is smaller than the Ekman drift predicted by that theory.

If this two-layer model were run to the steady state of thermocline setup, the streamfunction would be zero, the Ekman drift would be balanced by a geostrophic upper layer current and the lower layer

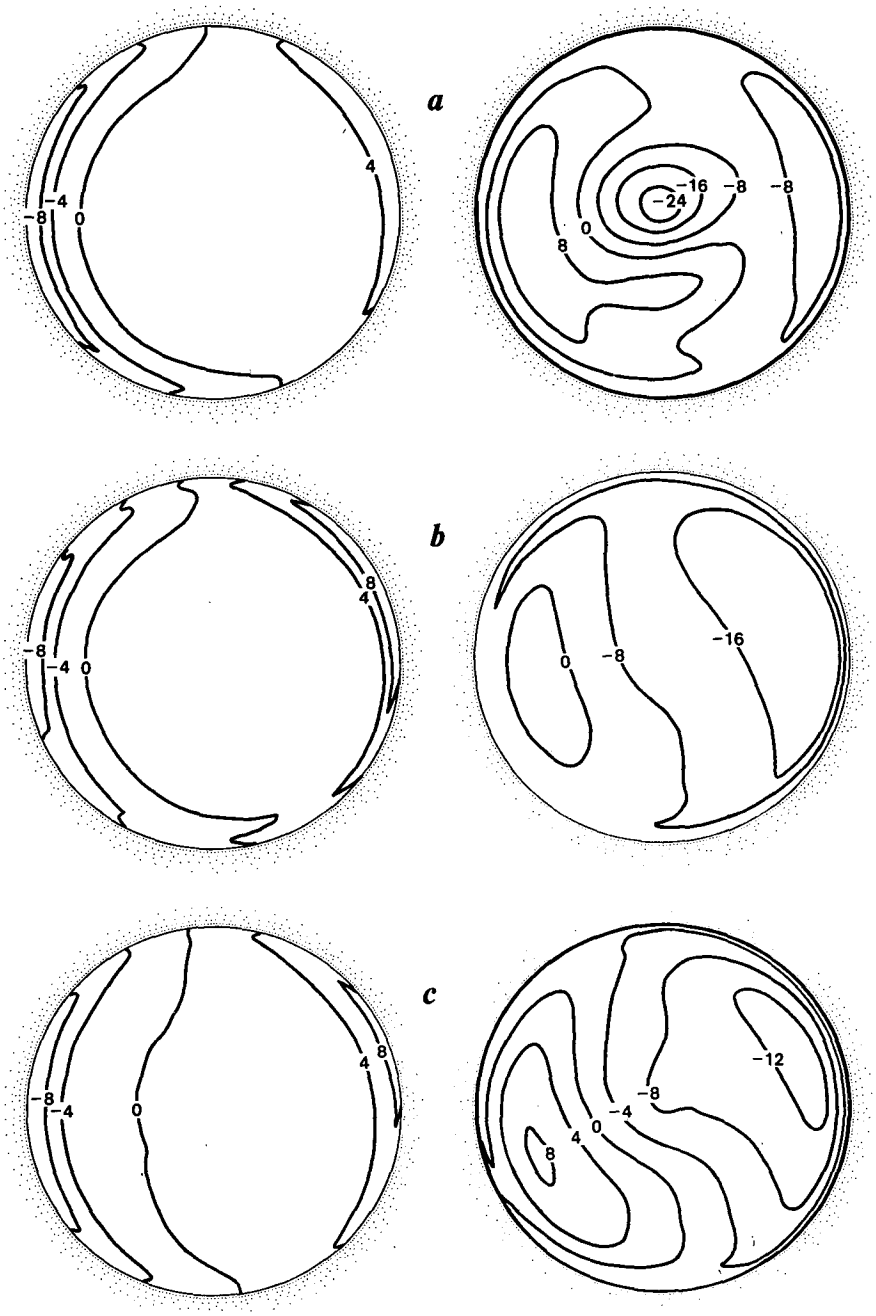

FIG. 5. Thermocline displacement (m) and streamfunction (10^9 cm^3 s^{-1}), 15 July to 15 August 1972, computed with both second-order thermocline displacements and the inertial acceleration terms for three values of friction d: (a) one-fourth of the bottom friction, (b) twice the bottom friction and (c) four times the interface friction.

current would be zero. Because for this figure the spindown is incomplete, the solution looks like a compromise between Birchfield's theory and the setup solution.

In the middle of Fig. 4 is the sum of the linear solution and the solution of the second-order problem driven by the terms depending on the displacement of the thermocline but without the inertial acceleration terms. This case is the most similar to the numerical model of Part I. As we expect from the simple model of Section 2, the upwelling is slightly larger than the downwelling and the cyclonic gyre is larger than the anticyclonic one.

The solution at the bottom of Fig. 4 includes both

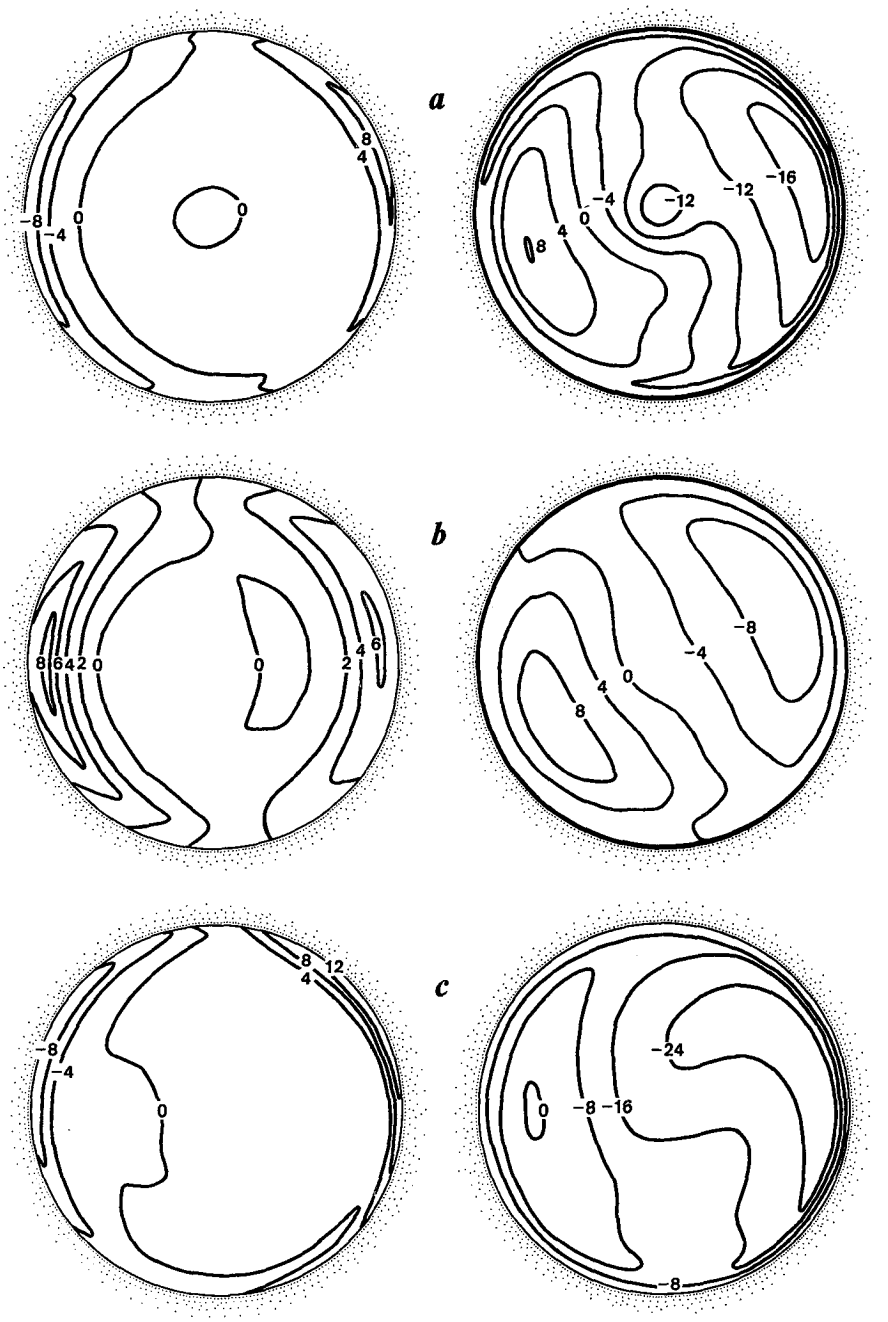

FIG. 6. Thermocline displacement (m) and streamfunction (10^9 cm^3 s^{-1}), 15 July to 15 August 1972, computed with both second-order thermocline displacements and inertial effects for the friction coefficients of Fig. 4 but with different grid resolution and smoothing: (a) no smoothing, (b) a uniform 7.5 km grid and (c) a stretched grid with four times the number of grid points.

finite-amplitude thermocline displacements and inertial accelerations. The addition of the inertial accelerations does not change the solution much for the values of friction and for the grid resolution used here. Near the center of the lake, however, there is a cyclonic curvature of the streamlines. The reason for this is the same as for the anticyclonic gyre caused by flow over a local rise in the seafloor in the theory of Huppert and Bryan (1976). At the extremum, the bottom slope is zero and small displacements of fluid do not cause vorticity to be generated by topographic stretching. To a second

approximation, however, the water at the center has to have come from a shallower depth and must therefore have a cyclonic vorticity.

Fig. 5 presents solutions to illustrate the effects of varying friction. First, at the top is the solution for a bottom friction coefficient of 0.005, one-fourth that of Fig. 4. For lower bottom friction the mean coastal flow is weaker, but the cyclonic flow in the center is stronger and forms a closed gyre. In the middle of the figure is the solution for twice the value of bottom friction (i.e., eight times the value of the solution above it). For this higher bottom friction, the flow is strongest in the coastal zone. The cyclonic gyre is stronger than in the bottom of Fig. 4 and the anticyclonic gyre is weaker. This can be understood from the logic of Section 2; the source of cyclonic angular momentum is the bottom stress.

At the bottom of Fig. 5 is the solution for four times the interface friction. Increasing the interface friction has the effect of decreasing the strength of the mean flow simply because it decreases the amplitude of the primary currents driving it.

The effects of the numerical method are examined in Fig. 6. At the top is the solution obtained by eliminating the smoothing. This solution is nearly identical to the bottom of Fig. 4. The reason the smoothing has little effect on the mean flow is that the linear motions driving it have long time scales compared to f^{-1}; thus most of the energy is in nondivergent motion and is little affected by the smoothing term (3.10) proportional to the horizontal divergence.

In the middle of Fig. 6 is the solution for the same parameters as the bottom of Fig. 4 but with a constant grid size of 7.5 km, 10 grid points between the center and the shore. The effect of decreasing the resolution is to lower the amplitude of the linear solution by spreading the boundary layer vertical motion over a wider zone. Thus, the mean thermocline pattern also has wider coastal zones and the streamfunction pattern is more symmetric. In this respect, decreasing resolution has an effect similar to that of increasing the interface friction coefficient.

Finally, at the bottom of Fig. 6 is the solution for a stretched grid of 72 points—four times that of Fig. 4, with minimum grid size of 0.4 km. The linear solution for this case, not shown here, is nearly identical to the top of Fig. 4; this is because the linear time-averaged solution does not have a boundary layer character. Increasing the resolution, however, has a large effect on the nonlinear terms. The major differences are that the cyclonic gyre is larger and the anticyclonic gyre is smaller. There is a narrow band of cyclonic flow at all parts of the shore. This fact is encouraging because the numerical model of Part I failed to reproduce the westward flow near the Oshawa shore. The circular model suggests that even better resolution may remedy this.

5. Summary

This paper concludes a three-part analysis of Lake Ontario's circulation for 15 July to 15 August 1972, a period of the International Field Year for the Great Lakes when detailed measurements were made. It is now appropriate to summarize all of them and to discuss some of the wider implications of the work.

The first paper (Bennett, 1977) pointed out some of the deficiencies of using a uniform 5 km grid model to compute the currents, discussed some of the possible reasons for them, and presented an alternative model that uses a variable grid resolution to resolve the coastal boundary layers. The uniform grid model has two major deficiencies. First, it fails to reproduce the fact that the mean current near the north shore is toward the west—opposite the wind. Second, it fails to reproduce the strength of the reversals of longshore current and thermocline displacement. Because linear models of both homogeneous and stratified lakes predict complex boundary layers, it is reasonable to expect that increased model resolution would help. The analysis of the stretched grid model supports this thesis.

The second paper (Bennett and Lindstrom, 1977) developed an empirical description of the flow in the coastal boundary layer. The mean flow is basically a geostrophic cyclonic gyre with weak currents below the thermocline and a 5 cm s^{-1} longshore current above the thermocline. The mean thermocline is depressed nearshore in accordance with geostrophic equilibrium. The deviations from this state were described by the solutions of wave equations driven by the longshore component of the wind stress. These linear equations admit very simple interpretations in terms of elementary momentum balances and coastal wave theories. Both the values of the wind forcing coefficients and the empirical decay times suggest that the basic approach of the numerical models is correct and that efforts to increase resolution and use lower friction coefficients would be fruitful.

Finally, in this paper I presented a simple nonlinear upwelling theory and a circular numerical model. This circular lake analogue was used to isolate the mechanisms operating in the more complicated model and to examine the importance of the physical parameters and the grid resolution. This model shows that the observed cyclonic mean flow is due to the rectified effects of the transient motion.

The effects of friction and resolution were shown to be quite complex. Reducing bottom friction tends to increase the magnitude of the cyclonic flow but to confine it to the central region. Further investigation of this effect has revealed that this aspect can be explained with a single-layer, rigid-lid model. This flow can be thought of as the rectified flow due to forced topographic waves. Both in-

creasing thermocline friction and increasing the grid size tend to reduce the magnitude of the baroclinic response and thus underestimate the effect of large thermocline displacements investigated with the simple model of Section 2.

The best agreement with the observed flow was obtained with the friction coefficients estimated from the observed decay times of the linear waves and with very high grid resolution. Thus, the basic conclusions of this work are that the transient features of Lake Ontario's currents can be explained by simple linear wave models and that the mean flow can be explained by the second-order effects of the waves. If these conclusions are correct, models that take into account the complex geometries of real lakes and require detailed estimates of atmospheric forcing are not necessary. If the effects of model grid resolution are as strong as shown here, such complex models may also be impossible. It would be worthwhile to test whether these conclusions are true for other lakes and to investigate both linear and second-order wave theories in more detail.

Acknowledgments. I thank Hsien Wang Ou and D. B. Rao for many interesting discussions. Most of this work was done at the Massachusetts Institute of Technology, where it was supported by the Great Lakes Environmental Research Laboratory under NOAA Contract 03-5-002-57 and by a grant from the Henry L. and Grace Doherty Charitable Foundation, Inc.

REFERENCES

Bennett, J. R., 1973: A theory of large-amplitude Kelvin waves. *J. Phys. Oceanogr.*, **3,** 57–60.

——, 1975a: Another explanation of the observed cyclonic circulation of large lakes. *Limnol. Oceanogr.*, **20,** 108–110.

——, 1975b: Nonlinearity of wind-driven currents. *Proc. Symp. Modeling of Transport Mechanisms in Oceans and Lakes*, Canada Centre for Inland Waters, Manuscript Rep. Ser. No. 43, Marine Science Directorate, Dept. of Fisheries and the Environment, Ottawa.

——, 1977: A three-dimensional model of Lake Ontario's summer circulation. I. Comparison with observations. *J. Phys. Oceanogr.*, **7,** 591–601.

——, and E. J. Lindstrom, 1977: A simple model of Lake Ontario's coastal boundary layer. *J. Phys. Oceanogr.*, **7,** 620–625.

Birchfield, G. E., 1972: Theoretical aspects of wind-driven currents in a sea or lake of variable depth with no horizontal mixing. *J. Phys. Oceanogr.*, **2,** 355–366.

Charney, J. G., 1955: Generation of oceanic currents by wind. *J. Mar. Res.*, **14,** 477–498.

Csanady, G. T., and J. T. Scott, 1974: Baroclinic coastal jets in Lake Ontario during IFYGL. *J. Phys. Oceanogr.*, **4,** 524–541.

Huppert, H. E., and K. Bryan, 1976: Topographically generated eddies. *Deep-Sea Res.*, **23,** 655–679.

Simons, T. J., 1975: Verification of numerical models of Lake Ontario. II. Stratified circulations and temperature changes. *J. Phys. Oceanogr.*, **5,** 98–110.

Williams, G. P., 1969: Numerical integration of the three-dimensional Navier Stokes equations for incompressible flow. *J. Fluid Mech.*, **37,** 727–750.